https://dx.doi.org/10.4314/bajopas.v19i1.12

BAYERO JOURNAL OF PURE AND APPLIED SCIENCES

Volume 19 Issue 1, June, 2026

Received: 10th April 2026 **Accepted:** 12th May 2026

ASSESSMENT OF *Chasmanthera dependens* (Hochst.) EXTRACT AND FRACTIONS ON ACETYLCHOLINESTERASE AND MONOAMINE OXIDASE ACTIVITIES

[1]Ikponmwosa-Eweka, O., [1]Ayeni, P. O., [2]Ogunyemi, A. T. and [3]Edogun, O.

[1]Department of Medical Biochemistry, School of Basic Medical Sciences, College of Medical Sciences, University of Benin, Benin City, Edo State, Nigeria.

[2]Medicine and Surgery Programme, College of Health Sciences, Bowen University, Iwo, Osun State, Nigeria.

3Department of Biochemistry, Faculty of Life Sciences, University of Benin, Benin City, Edo State, Nigeria.

*Corresponding author: E-mail address: peluola.ayeni@uniben.edu

Abstract

Chasmanthera dependens is traditionally used for managing neurodegenerative disorders. This study evaluated the acetylcholinesterase (AChE) and monoamine oxidase (MAO) inhibitory activities of *C. dependens* root fractions, and also investigated the binding mechanisms of its phytoconstituents against AChE and MAO-B through molecular docking. Crude methanol extract and fractions (dichloromethane, ethyl acetate, and butanol) of *C. dependens* root were assessed for *in vitro* inhibitory effects against AChE and MAO activities using spectrophotometric methods. Molecular docking simulations were performed using AutoDock Vina to predict binding affinities and interaction modes of identified compounds with AChE and MAO-B active sites. All fractions demonstrated significant enzyme inhibitory activities. For AChE inhibition, all fractions exhibited IC_{50} values comparable to donepezil, with no significant differences observed ($p > 0.05$). For MAO inhibition, the methanol fraction demonstrated significantly higher activity than donepezil, while ethyl acetate and butanol fractions showed comparable activity to the standard. Molecular docking against MAO-B revealed that kaempferol exhibited the strongest binding affinity among the phytochemicals, approaching that of donepezil (−11.2 Kcal/mol). Catechin (−9.4 Kcal/mol), ellagic acid (−9.1 Kcal/mol), and resveratrol (−9.0 Kcal/mol) also demonstrated favorable binding energies, while chlorogenic acid (−8.9 Kcal/mol) and rutin (−7.8 Kcal/mol) showed moderate binding. For AChE, ellagic acid (−9.8 Kcal/mol) and catechin (−9.2 Kcal/mol) exhibited strong binding affinities with favorable interactions at key amino acid residues including Trp84, Phe330, and Tyr334. This study provides scientific evidence supporting the neuroprotective potential of *C. dependens* through multiple mechanisms including AChE inhibition and MAO-B inhibition.

Keywords: *Chasmanthera dependens*, acetylcholinesterase, monoamine oxidase B, lipid peroxidation, molecular docking

INTRODUCTION

Neurodegenerative disorders such as Alzheimer's disease (AD) and Parkinson's disease (PD) are increasing globally with aging populations (Debiec and Rojek, 2026). Alzheimer's disease affects about 50 million people worldwide, while Parkinson's disease affects over 10 million (Zhang *et al*., 2025). These conditions are characterized by progressive neuronal loss, cognitive and motor impairment, and substantial socio-economic burden. Their pathogenesis is multifactorial. In Alzheimer's disease, reduced cholinergic neurotransmission due to degeneration of basal forebrain neurons underlies cognitive decline (Geula *et al*., 2021). Acetylcholinestease (AChE) hydrolyzes acetylcholine in the synaptic cleft, and its inhibition enhances cholinergic signaling; consequently, AChE inhibitors such as donepezil, rivastigmine, and galantamine remain first-line therapies (Nagori *et al*., 2024). In Parkinson's disease, monoamine oxidase (MAO) contributes to dopamine degradation and oxidative stress; selective MAO inhibition preserves dopaminergic transmission and improves motor symptoms (Sagura-Aguilar and Paris, 2022; Naoi *et al*., 2024). MAO activity also generates hydrogen peroxide, linking neurotransmitter metabolism to oxidative damage (Behl *et al*., 2021). Oxidative stress is a central feature across neurodegenerative disorders. The brain's high oxygen consumption, lipid-rich composition, and relatively limited antioxidant defenses make it particularly vulnerable (Serban *et al*., 2025). Lipid peroxidation produces reactive aldehydes such as malondialdehyde, which impair membrane integrity and neuronal function (Petrovic *et al*., 2020), and elevated levels have been reported in AD and PD patients (Allowitz *et al*., 2024).Given the interplay between cholinergic dysfunction, monoamine metabolism, and oxidative stress, multi-target therapeutic approaches may offer advantages over single-target strategies (Verma, 2025). Medicinal plants, rich in diverse bioactive compounds, represent promising sources of such interventions (Chintada and Golla, 2025).

Chasmanthera dependens (Menispermaceae) is a climbing shrub widely distributed in tropical Africa (Salawu *et al*., 2025). Traditionally used for fever, malaria, and other ailments (Tijani *et al*., 2022), it has also been reported in Nigerian ethnomedicine for managing memory loss and age-related cognitive decline (Jabba *et al*., 2025; Hounsou *et al*., 2026). This study therefore evaluated the *in vitro, ex-vivo and in-silico* AChE and MAO inhibitory activities of crude extract and fractions of *C. dependens* root and investigated the binding interactions of selected phytochemicals (rutin, kaempferol, resveratrol, ellagic acid, catechin, and chlorogenic acid) with AChE and MAO-B using molecular docking techniques.

MATERIALS AND METHODS

Plant Material Collection and Authentication

Fresh roots of *Chasmanthera dependens* were collected from natural habitats in Edo State, Nigeria. Taxonomic identification and authentication were performed by a botanist at the Department of Plant Biology and Biotechnology, University of Benin, Nigeria. A voucher specimen (UBHC387) was deposited at the University Herbarium for future reference.

Preparation of Crude Extract

The collected roots were thoroughly washed and air-dried at room temperature (25 ± 2°C) for 14 days. The dried material was pulverized into fine powder using an electric grinder. Powdered root material (2.5 kg) was macerated in 7.5 L of absolute methanol for 72 h at room temperature with intermittent agitation (Dagdag *et al.*, 2024). The mixture was filtered through Whatman No. 1 filter paper, and the residue was re-extracted twice with fresh methanol to ensure exhaustive extraction. Combined filtrates were concentrated under reduced pressure at 40°C using a rotary evaporator (Buchi R-300, Switzerland). The resulting crude methanol extract (CME) was weighed, transferred to airtight containers, and stored at 4°C until further analysis.

Fractionation by Vacuum Liquid Chromatography

The crude methanol extract (320 g) was subjected to vacuum liquid chromatography (VLC) for fractionation. A glass column (10 cm × 30 cm) was packed with Merck grade silica gel (70–230 mesh) under vacuum to create a uniform stationary phase. The extract was adsorbed onto a small quantity of silica gel, dried, and carefully layered on top of the column. Stepwise gradient elution was performed using solvents of increasing polarity: 100% dichloromethane, 100% ethyl acetate, and 100% butanol. Each fraction was collected separately, and the process was monitored by thin-layer chromatography (TLC) using appropriate solvent systems. Fractions showing similar TLC profiles were pooled. The collected fractions dichloromethane fraction (DCM-F), ethyl acetate fraction (EA-F), and butanol fraction (BUT-F) were evaporated to dryness under reduced pressure.

Chemicals and Reagents

Acetylthiocholine iodide, 5,5'-dithio-bis(2-nitrobenzoic acid) (DTNB), benzylamine, sodium nitroprusside (SNP), thiobarbituric acid (TBA), sodium dodecyl sulfate (SDS), donepezil, and all other analytical grade chemicals and solvents were procured from Sigma-Aldrich (St. Louis, MO, USA). Phosphate buffer saline and other reagents were obtained from Merck (Darmstadt, Germany). Donepezil hydrochloride was purchased from Care yard pharmacy, Iwo, Osun state, Nigeria.

Preparation of Brain Homogenate

Adult Wistar rats (200–250 g) were obtained from the Animal House of the Department of Biochemistry, University of Benin, Nigeria. Animals were maintained under standard laboratory conditions (12-hour light/dark cycle, 25 ± 2°C) with free access to standard pellet diet and water ad libitum. All procedures followed the guidelines for the care and use of laboratory animals and were approved by the Institutional Animal Ethics Committee. Rats were euthanized by cervical dislocation, and whole brains were rapidly dissected, washed in ice-cold 0.1 M phosphate buffer (pH 7.4), and homogenized in 5 volumes (w/v) of the same buffer using a Teflon-glass homogenizer. The homogenate was centrifuged at 3000 rpm for 10 minutes at 4°C to obtain the supernatant (S1 fraction), which was used for enzyme inhibition and lipid peroxidation assays.

Lipid Peroxidation and Malondialdehyde (MDA) Inhibition Assay

5 mM of newly made sodium nutoprusside (SNP), 0.1 M Tris-HCl buffer solution (pH 7.4), different quantities of the Chasmanthera dependens extract (0–100 µL), and 100 µL of the S1 brain homogenate were combined to create a reaction mixture. The reaction mixture was incubated at 37 °C for one hour after distilled water was added to bring the total volume to 300 µL. The reaction tubes were then filled with 300 µL of 8.1% sodium dodecyl sulfate (SDS), 600 µL of acetic acid/HCl solution (pH 3.4), and 600 µL of 0.8% thiobarbituric acid (TBA) solution. To produce color, the mixture was incubated at 100 °C for one hour. A UV-Visible spectrophotometer was used to test the generated pink chromogen's absorbance at 532 nm after it had cooled. A standard curve of malondialdehyde (MDA) was used to calibrate the degree of lipid peroxidation (Ayeni *et al.*,2025).

Acetylcholinesterase (AChE) Inhibition Assay

The extract's inhibitory effects on acetylcholinesterase (AChE) activity were assessed using a modified colorimetric method developed by Adefegha *et al.*, (2021). The reaction mixture consisted of 50 µL of homogenate solution in 0.1 M phosphate buffer at pH 8.0, 50 µL of 3.3 mM 5,5-dithio-bis (2 nitrobenzoic acid) in 0.1 M phosphate buffer solution at pH 7.0 with 6 mM NaHCO3, and 50–150 µL of the extracts. AChE activity was assessed using UV spectrophotometry based on changes in absorbance at 412 nm for 3.0 minutes following 20 minutes of incubation at 25 °C using acetylthiocholine iodide (100 mL of 0.05 mM water solution) as the substrate. The % inhibition was calculated to express the extract's inhibitory effects on AChE.

Monoamine Oxidase (MAO) Inhibition Assay

A modified colorimetric approach was used to evaluate monoamine oxidase inhibition, as detailed by Adefegha *et al.* (2021). 75 µL of homogenate, 10 mMMm benzylamine (pH 7.0), 0.025 M phosphate buffer (pH 7), and 0.0125 M semicarbazide were combined to evaluate MAO activity. After that, the combination was left to incubate for half an hour. The addition of acetic acid was followed by a three-minute boil. The next step was to add 0.05% of 2, 4-dinitrophenyl hydride (DNPH). 0.1 M NaOH was added to the mixture after it had been incubated for ten minutes at 25 °C.

Molecular Docking Studies

Three-dimensional structures of bioactive compounds identified in *C. dependens* rutin, kaempferol, resveratrol, ellagic acid, catechin, and chlorogenic acid were obtained from the PubChem database

(https://pubchem.ncbi.nlm.nih.gov/). Donepezil served as the reference drug. Ligands were energy-minimized using the Merck Molecular Force Field (MMFF94) and converted to PDBQT format using Open Babel (Ullah *et al.*, 2024).

Crystal structures of acetylcholinesterase (*Torpedo californica*, PDB ID: 1EVE) and human monoamine oxidase B (PDB ID: 2V5Z) were retrieved from the RCSB Protein Data Bank. Water molecules and co-crystallized ligands were removed, polar hydrogens were added, and Kollman charges were assigned using AutoDock Tools (Golj *et al.*, 2025).

Molecular docking was performed using AutoDock Vina (Che *et al.*, 2023) with a grid box of 30 × 30 × 30 Å centered on the active sites. Nine conformations were generated for each ligand, and the pose with the lowest binding energy was selected. Docking interactions were analyzed using Discovery Studio Visualizer to identify hydrogen bonding and hydrophobic interactions within the enzyme active sites.

Statistical Analysis

All experimental data were expressed as mean ± standard error of the mean (SEM) of triplicate determinations. Statistical analyses were performed using GraphPad Prism version 8.0.2 (GraphPad Software, San Diego, CA, USA). IC_{50} values were calculated by linear regression analysis. Differences were considered statistically significant at $p \leq 0.05$. Values with the same alphabetical superscripts in tables indicate no significant difference.

RESULTS

Inhibition of Lipid Peroxidation (MDA Inhibition)

The inhibitory effects of *C. dependens* fractions against SNP-induced lipid peroxidation in rat brain homogenates are presented in Figure 1. All tested fractions demonstrated concentration-dependent inhibition of MDA formation.

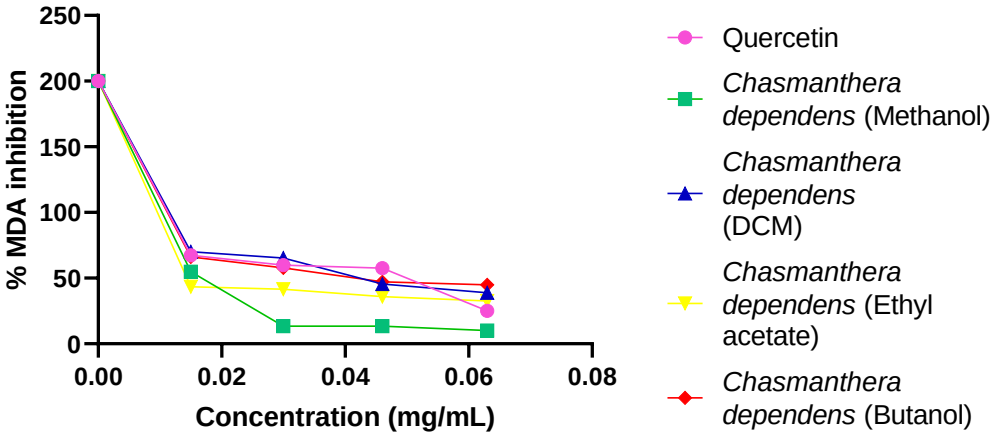

Figure 1: Percentage MDA Inhibition by Various Fractions of *Chasmanthera dependens*
Bars represent mean ± SEM (n=3) of duplicate determinations.

The IC_{50} values for lipid peroxidation inhibition are presented in Table 1. The butanol fraction exhibited the lowest IC_{50} (0.047 mg/mL), indicating the highest potency, followed closely by the dichloromethane fraction (0.048 mg/mL) and donepezil (0.051 mg/mL). The ethyl acetate fraction showed an IC_{50} of 0.064 mg/mL, while the methanol extract had the highest IC_{50} (0.146 mg/mL), indicating the lowest potency.

Table 1: IC_{50} of *Chasmanthera dependens'* Effect on SNP-Induced Lipid peroxidation in rat brain (mg.mL)

Sample	IC_{50} Values
Control	0.051 ± 0.002^{a}
Chasmanthera dependens (Methanol)	0.146 ± 0.005^{b}
Chasmanthera dependens (DCM)	0.048 ± 0.002^{a}
Chasmanthera dependens (Ethyl acetate)	0.064 ± 0.003^{c}
Chasmanthera dependens (Butanol)	0.047 ± 0.003^{d}

Values represents mean ± SEM (n=3), representing means of duplicates. Values are statistically different at $p \leq 0.05$. Values with the same alphabet are not significantly different.

Statistical analysis revealed that the butanol and dichloromethane fractions showed significantly higher activity (lower IC_{50}) compared to the methanol extract ($p < 0.001$) and ethyl acetate fraction ($p < 0.05$). Notably, the butanol and dichloromethane fractions exhibited IC_{50} values comparable to donepezil, with no significant differences observed ($p > 0.05$). The ethyl acetate fraction showed significantly lower activity than donepezil ($p < 0.05$).

Acetylcholinesterase (AChE) Inhibition

The AChE inhibitory activities of *C. dependens* fractions are illustrated in Figure 2. All fractions demonstrated concentration-dependent inhibition of AChE activity.

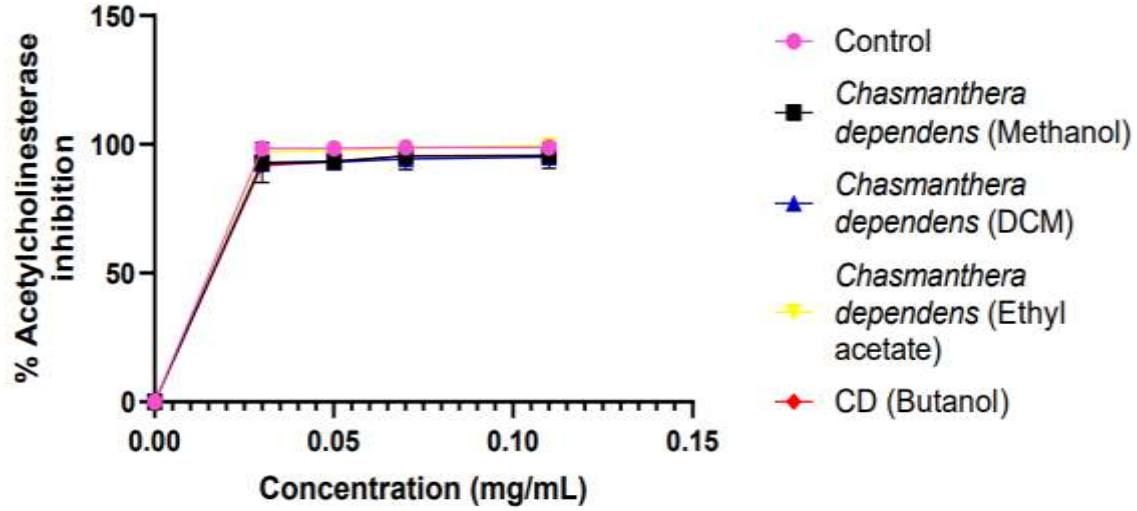

Figure 2: Percentage AChE Inhibition by Various Fractions of *Chasmanthera dependens*
Bars represent mean ± SEM (n=3) of duplicate determinations.

The IC_{50} values for AChE inhibition are presented in Table 2. All tested samples showed excellent AChE inhibitory activity with IC_{50} values ranging from 0.039 to 0.041 mg/mL. Donepezil, the standard drug, exhibited an IC_{50} of 0.039 mg/mL. The ethyl acetate fraction matched this value exactly (0.039 mg/mL), while the methanol extract, dichloromethane fraction, and butanol fraction each showed IC_{50} values of 0.041 mg/mL.

Table 2: IC_{50} of AChE inhibitory abilities of *Chasmanthera dependens* fractions (mg/mL)

Sample	IC_{50} Values
Donepezil	0.039 ± 0.002[a]
Chasmanthera dependens (Methanol)	0.041 ± 0.002[a]
Chasmanthera dependens (DCM)	0.041 ± 0.002[a]
Chasmanthera dependens (Ethyl acetate)	0.039 ± 0.002[a]
Chasmanthera dependens (Butanol)	0.041 ± 0.002[a]

Values represents mean ± SEM (n=2), representing means of duplicates. Values are statistically different at $p \leq 0.05$. Values with the same alphabet are not significantly different.

Acetylcholinesterase enzyme was inhibited by the fractions of *Chasmanthera dependens* in concentration dependent manner however, as revealed by their IC_{50} values, there were no significant differences among them when compared to the donepezil control. Statistical analysis revealed no significant differences among any of the tested samples and donepezil ($p > 0.05$), indicating that all fractions of *C. dependens* possess AChE inhibitory activity comparable to the standard drug.

Monoamine Oxidase (MAO) Inhibition

The MAO inhibitory activities of *C. dependens* fractions are presented in Figure 3. Concentration-dependent inhibition of MAO activity was observed for all fractions.

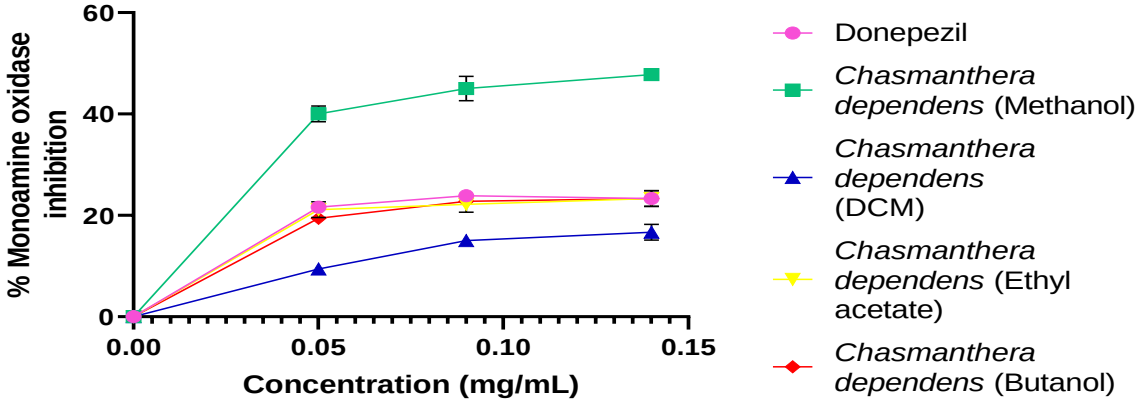

Figure 3: Percentage MAO Inhibition by Various Fractions of *Chasmanthera dependens*
Bars represent mean ± SEM (n=2) of duplicate determinations.

The IC_{50} values for MAO inhibition are presented in Table 3. The methanol fraction exhibited the lowest IC_{50} (0.119 mg/mL), indicating the highest potency, significantly exceeding that of donepezil (0.233 mg/mL). The ethyl acetate fraction (0.239 mg/mL) and butanol fraction (0.240 mg/mL) showed IC_{50} values comparable to donepezil. The dichloromethane fraction exhibited the highest IC_{50} (0.363 mg/mL), indicating the lowest potency.

Table 3: IC_{50} of MAO inhibitory abiloties of *Chasmanthera dependens* fractions (mg/mL)

Sample	IC_{50} Values
Donepezil	0.233 ± 0.005^{a}
Chasmanthera dependens (Methanol)	0.119 ± 0.005^{b}
Chasmanthera dependens (DCM)	0.363 ± 0.005^{c}
Chasmanthera dependens (Ethyl acetate)	0.239 ± 0.005^{a}
Chasmanthera dependens (Butanol)	0.240 ± 0.005^{a}

Values represents mean ± SEM (n=2), representing means of duplicates. Values are statistically different at $p \leq 0.05$. Values with the same alphabet are not significantly different.

Statistical analysis revealed that the methanol fraction showed significantly higher MAO inhibitory activity (lower IC_{50}) compared to donepezil ($p < 0.001$), ethyl acetate fraction ($p < 0.001$), and butanol fraction ($p < 0.001$). The dichloromethane fraction exhibited significantly lower activity (higher IC_{50}) than all other samples ($p < 0.001$). No significant differences were observed among donepezil, ethyl acetate fraction, and butanol fraction ($p > 0.05$).

Molecular Docking Results
Binding Affinities Against MAO-B
Molecular docking simulations were performed to predict the binding affinities of six phytochemicals from *C. dependens* against human monoamine oxidase B (MAO-B). Donepezil was included as reference. The calculated binding energies (Kcal/mol) are presented in Table 4.

Table 4: Binding Energies of Phytochemicals from *C. dependens* against Monoamine Oxidase B (MAO-B)

S/N	Phytochemical	MAO-B Binding Energy (Kcal/mol)
1	Rutin	-7.8
2	Kaempferol	-10.5
3	Resveratrol	-9.0
4	Ellagic Acid	-9.1
5	Catechin	-9.4
6	Chlorogenic acid	-8.9
7	Donepezil (Standard Drug)	-11.2

All tested phytochemicals demonstrated favorable binding energies (more negative than −7.5 Kcal/mol) with MAO-B, indicating spontaneous binding. Kaempferol exhibited the strongest binding affinity among the phytochemicals (−10.5 Kcal/mol), approaching that of donepezil (−11.2 Kcal/mol). Catechin (−9.4 Kcal/mol), ellagic acid (−9.1 Kcal/mol), and resveratrol (−9.0 Kcal/mol) also demonstrated strong binding affinities. Chlorogenic acid (−8.9 Kcal/mol) showed moderate binding, while rutin (−7.8 Kcal/mol) exhibited the weakest binding among the tested compounds.

Ligand-Protein Interaction Analysis for MAO-B

Detailed analysis of ligand-enzyme interactions revealed the molecular basis for the observed binding affinities. Figures 4 and 5 presents the 2D interaction diagrams and 3D surface views for all phytochemicals with the MAO-B active site.

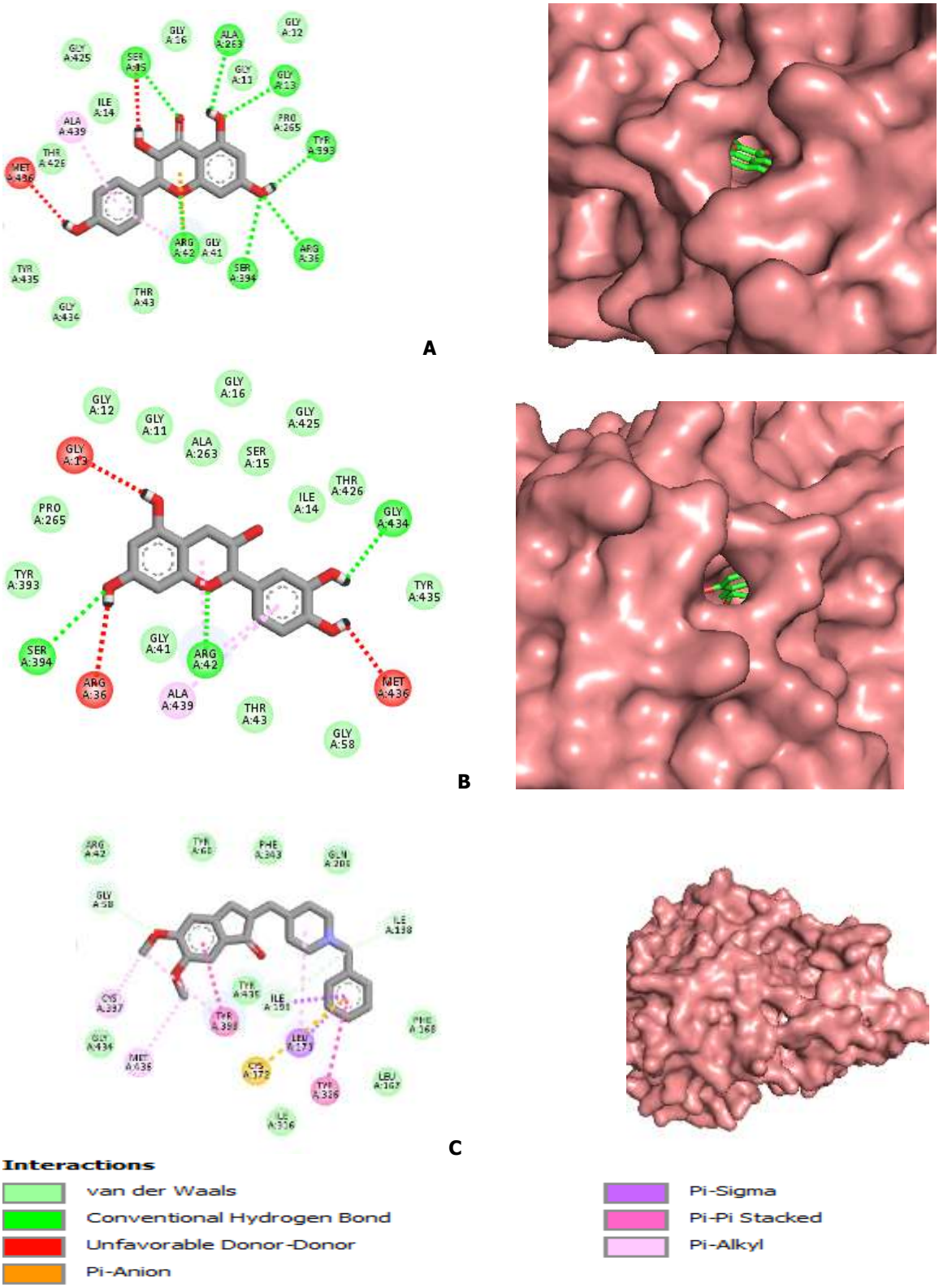

Figure 4: 2D and 3D ligand interaction of (A) Kaemferol, (B) Catechin and (C) Donepezil with the amino acid residues within the binding pockets of Monoamieoxidase

Table 5: Binding Energies of Bioactive Compounds from *C. dependens* against Acetylcholinesterase (AChE)

S/N	Phytochemical	AChE Binding Energy (Kcal/mol)
1	Ellagic Acid	-9.8
2	Catechin	-9.2
3	Donepezil (Standard drug)	-11.5

Both ellagic acid and catechin demonstrated favorable binding energies with AChE, with ellagic acid (−9.8 Kcal/mol) showing stronger binding than catechin (−9.2 Kcal/mol).

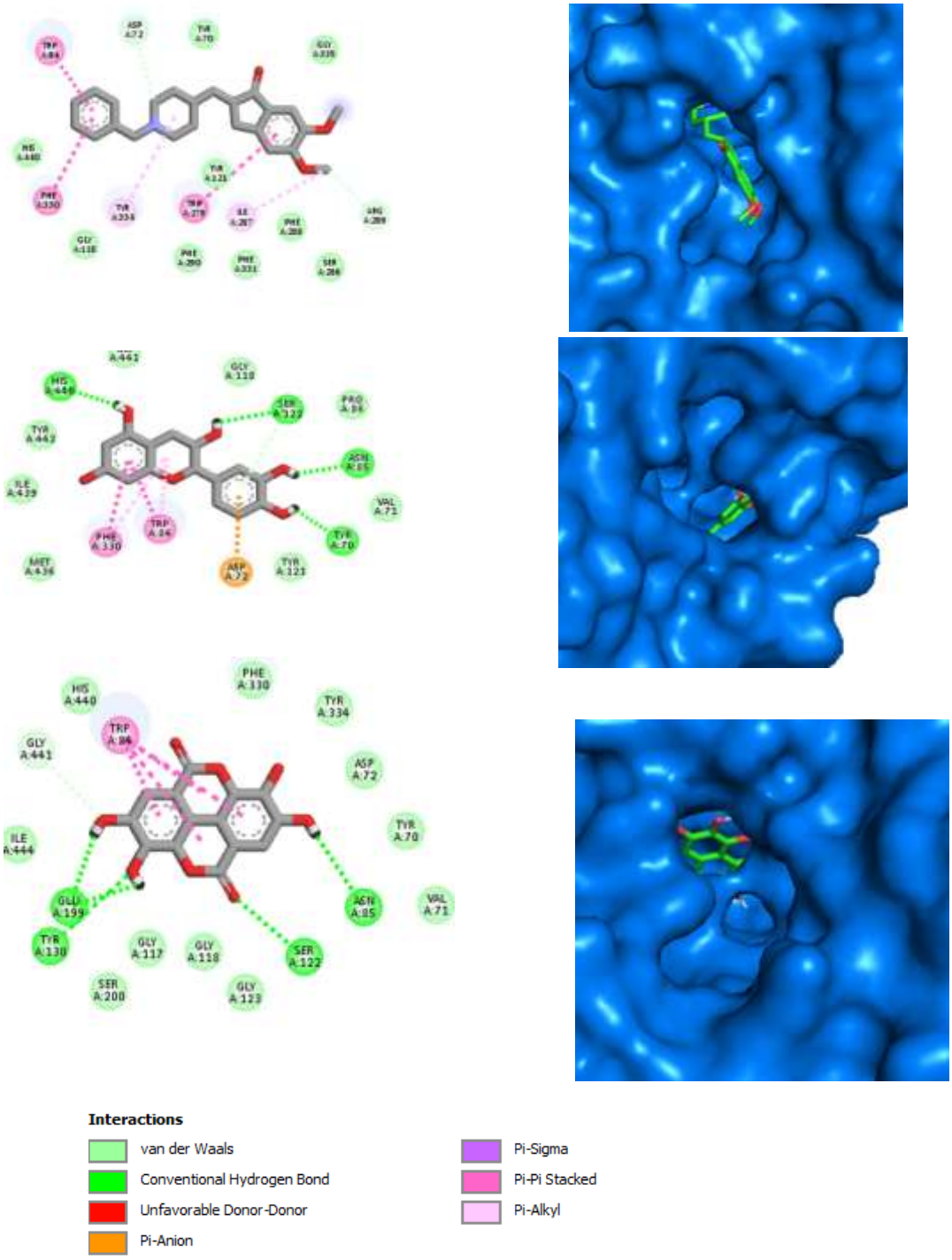

Figure 5: 2D and 3D ligand interaction of (A) Ellagic acid, (B) Catechin and (C) Donepezil with the amino acid residues within the binding pockets of acetylcholinesterase

DISCUSSION

The present study evaluated the acetylcholinesterase (AChE) and monoamine oxidase (MAO) inhibitory activities and anti-lipid peroxidation effects of *Chasmanthera dependens* root fractions using combined *in vitro*, *ex-vivo* and *in silico* approaches. The results indicate that the plant contains bioactive compounds capable of targeting multiple mechanisms associated with neurodegeneration, supporting its traditional use in neurological disorders.

The butanol (IC_{50} = 0.047 mg/mL) and dichloromethane (IC_{50} = 0.048 mg/mL) fractions showed strong inhibition of sodium nitroprusside-induced lipid peroxidation, with IC_{50} values comparable to donepezil (IC_{50} = 0.051 mg/mL) in table 1. Lipid peroxidation is a major contributor to neuronal damage because the brain is highly susceptible to oxidative stress due to its high polyunsaturated fatty acid content (Angelova *et al*., 2021). The observed reduction in malondialdehyde formation suggests that the fractions possess significant antioxidant properties. The high activity of the butanol fraction may be attributed to glycosylated flavonoids and other phenolic compounds known for radical-scavenging ability (Zheng et al., 2025).

All fractions demonstrated strong AChE inhibitory activity comparable to donepezil, with the ethyl acetate fraction (IC_{50} = 0.039 mg/mL) showing the highest activity as revealed in the IC_{50} values in table 2. This suggests the presence of active phenolic compounds such as ellagic acid and catechin, which were also supported by molecular docking results showing strong binding interactions with key residues in the AChE active site. AChE inhibition enhances cholinergic neurotransmission and remains a primary therapeutic strategy for Alzheimer's disease (Yang *et al*., 2023).

The methanol fraction (IC_{50} = 0.119 mg/mL) exhibited the strongest MAO inhibitory activity, exceeding that of donepezil (IC_{50} = 0.233 mg/mL) as shown in table 3. Docking analysis identified kaempferol as the compound with the highest binding affinity toward MAO-B, consistent with previous reports of flavonoids as MAO inhibitors (Adewole *et al*., 2022; Das *et al*., 2026). Since MAO-B contributes to dopamine degradation and oxidative stress in the brain, its inhibition is beneficial in Parkinson's disease management (Oyovwi *et al*., 2026).

Overall, the fractions demonstrated multi-target neuroprotective potential, combining AChE inhibition, MAO inhibition, and antioxidant activity. Such multi-target actions are desirable for complex neurodegenerative diseases like Alzheimer's and Parkinson's disease, which involve multiple pathological pathways (Toader *et al*., 2024; Katsoulaki *et al*., 2025). The differential activities of the fractions likely reflect their phytochemical composition, with flavonoids and phenolic acids playing key roles.

These findings are consistent with previous studies reporting antioxidant properties of *C. dependens* and related Menispermaceae species (Karau *et al*., 2021). However, this study provides additional evidence linking the plant to enzyme-based neuroprotective mechanisms. Despite these promising results, further studies using purified compounds, human enzymes, and ***in vivo*** models are necessary to validate the therapeutic potential of *C. dependens* in neurodegenerative disease management.

CONCLUSION

This integrated *in vitro* and *in silico* study suggests that *Chasmanthera dependens* root possesses notable neuroprotective potential, with fractions demonstrating anti-lipid peroxidation and AChE inhibitory activities comparable to donepezil, while the methanol fraction showed relatively stronger MAO inhibition. Molecular docking further indicates that kaempferol, ellagic acid, and catechin may contribute to these effects, highlighting the plant as a promising candidate for further investigation in neurodegenerative disorders.

Acknowledgements

The authors acknowledge the technical staff of the Department of Medical Biochemistry, University of Benin and Biochemistry Programme, Bowen University, Iwo, for laboratory assistance. This research did not receive any specific grant from funding agencies in the public, commercial, or not-for-profit sectors.

REFERENCES

Adefegha, S. A., Omojokun, O. S., Oboh, G., Fasakin, O., & Ogunsuyi, O. (2021). Modulator effects of ferulic acid on cadmium-induced brain damage. *Journal of Food Biochemistry, 45*(3), e13423.

Adewole, K. E., Gyebi, G. A., Ishola, A. A., & Falade, A. O. (2022). Computer-aided identification of cholinergic and monoaminergic inhibitory flavonoids from *Hibiscus sabdariffa* L. *Current Drug Discovery Technologies, 19*(5), 49–64.

Allowitz, K., Taylor, J., Harames, K., Yoo, J., Baloch, O., & Ramana, K. V. (2024). Oxidative stress-mediated lipid peroxidation-derived lipid aldehydes in the pathophysiology of neurodegenerative diseases. *Current Neuropharmacology*.

Angelova, P. R., Esteras, N., & Abramov, A. Y. (2021). Mitochondria and lipid peroxidation in the mechanism of neurodegeneration: Finding ways for prevention. *Medicinal Research Reviews, 41*(2), 770–784.

Ayeni, P. O., Sajere, E. O., Akanbi, C. A., Ayomipo, M. A., Sunday, D. J., & Ogunlakin, A. D. (2025). Combinative effects of kaempferol and quercetin on α-amylase and iron-induced lipid peroxidation in rat pancreas. *Journal of Phytomedicine and Therapeutics, 24*(2), 2500.

Behl, T., Kaur, D., Sehgal, A., Singh, S., Sharma, N., Zengin, G., Andronie-Cioara, F. L., Toma, M. M., Bungau, S., & Bumbu, A. G. (2021). Role of monoamine oxidase activity in Alzheimer's disease: An insight into the therapeutic

potential of inhibitors. *Molecules, 26*(12), 3724.

Che, X., Liu, Q., & Zhang, L. (2023). An accurate and universal protein-small molecule batch docking solution using AutoDock Vina. *Results in Engineering, 19*, 101335.

Chintada, V., & Golla, N. (2025). Exploring the therapeutic potential of bioactive compounds from plant sources. In *Biotechnological intervention in production of bioactive compounds: Biosynthesis, characterization and applications* (pp. 229–247). Springer Nature Switzerland.

Dagdag, O., Kim, H., Haldhar, R., Daoudi, W., & Berdimurodov, E. (2024). Phytochemicals/plant extracts: Preparation, characterization, and properties. In *Phytochemistry in corrosion science* (pp. 20–36). CRC Press.

Das, A., Bhuyan, P., & Ganguly, M. (2026). In silico pharmacological evaluation of berry polyphenols targeting monoamine oxidase-B in Parkinson's disease. *ChemistrySelect, 11*(11), e06861.

Dębiec, M., & Rojek, M. (2026). Adult neurogenesis in neurodegenerative diseases: Mechanisms of dysregulation in Alzheimer's and Parkinson's disease. *International Journal of Molecular Sciences, 27*(6), 2742.

Geula, C., Dunlop, S. R., Ayala, I., Kawles, A. S., Flanagan, M. E., Gefen, T., & Mesulam, M. M. (2021). Basal forebrain cholinergic system in the dementias: Vulnerability, resilience, and resistance. *Journal of Neurochemistry, 158*(6), 1394–1411.

Golj, D. R., Dinka, M. O., Sherefedin, U., Belay, A., Gelanu, D., & Megersa, G. D. (2025). Solvent polarity effects on the FTIR spectrum and thermodynamic and electronic properties of metronidazole and its binding with antibacterial drugs: A DFT and molecular docking study. *RSC Advances, 15*(35), 28538–28554.

Hounsou, K. E., Akande, M. D., Sonibare, M. A., Elufioye, T. O., Oyagbemi, A. A., & Olopade, F. E. (2026). Development and assessment of a synergy-based combined extracts of *Spondias mombin* L., *Spilanthes filicaulis* (Schumach. & Thonn.) C. D. Adams and *Piper guineense* Thonn. for learning and memory enhancement. *Current Trends in Biotechnology & Pharmacy, 20*(1), 2704.

Jabba, H. L., Dimeji, I. Y., Ayodeji, A. S., Baba, Z. M., Adeoye, S. W., & Olawale, A. S. (2025). *Tropical Journal of Natural Product Research*.

Karau, G. M., Njagi, E. N. M., Machocho, A. K., & Wangai, L. N. (2021). Antioxidant activity and phytochemical composition of selected medicinal plants of the Menispermaceae family. *Journal of Medicinal Plants Research, 15*(2), 85–94.

Katsoulaki, E. E., Dimopoulos, D., & Hadjipavlou-Litina, D. (2025). Multitarget compounds designed for Alzheimer, Parkinson, and Huntington neurodegeneration diseases. *Pharmaceuticals, 18*(6), 831.

Nagori, K., Pradhan, M., Sharma, M., Ajazuddin, Badwaik, H. R., & Nakhate, K. T. (2024). Current progress on central cholinergic receptors as therapeutic targets for Alzheimer's disease. *Current Alzheimer Research, 21*(1), 50–68.

Naoi, M., Maruyama, W., Shamoto-Nagai, M., & Riederer, P. (2024). Toxic interactions between dopamine, α-synuclein, monoamine oxidase, and genes in mitochondria of Parkinson's disease. *Journal of Neural Transmission, 131*(6), 639–661.

Oyovwi, M. O., Udi, O. A., Atere, A. D., Joseph, G. U., & Ogbutor, U. G. (2025). Molecular pathways: The quest for effective MAO-B inhibitors in neurodegenerative therapy. *Molecular Biology Reports, 52*(1), 240.

Petrovic, S., Arsic, A., Ristic-Medic, D., Cvetkovic, Z., & Vucic, V. (2020). Lipid peroxidation and antioxidant supplementation in neurodegenerative diseases: A review of human studies. *Antioxidants, 9*(11), 1128.

Salawu, K. M., Balogun, Q. O., Sulaiman, H. O., Ologe, M. F., & Salawu, O. O. (2025). Pharmacognostical evaluation, growth inhibitory and antioxidant activities of *Chasmanthera dependens* Hochst. *HAYATI Journal of Biosciences, 32*(4), 1010–1024.

Segura-Aguilar, J., & Paris, I. (2022). Mechanisms of dopamine oxidation and Parkinson's disease. In *Handbook of neurotoxicity* (pp. 1–36). Springer International Publishing.

Șerban, M., Toader, C., & Covache-Busuioc, R. A. (2025). The redox revolution in brain medicine: Targeting oxidative stress with AI, multi-omics and mitochondrial therapies for the precision eradication of neurodegeneration. *International Journal of Molecular Sciences, 26*(15), 7498.

Tijani, S. A., Akin-Akanbi, B. F., & Adeoye, B. O. (2022). Differential roles of tannin-rich extract of *Chasmanthera dependens* in modulating piroxicam induced electrolyte imbalance in rats. *European Journal of Pharmaceutical and Medical Research, 9*(8), 474–482.

Toader, C., Tataru, C. P., Munteanu, O., Serban, M., Covache-Busuioc, R. A., Ciurea, A. V., & Enyedi, M. (2024). Decoding neurodegeneration: A review of molecular mechanisms and therapeutic advances in Alzheimer's, Parkinson's, and ALS. *International Journal of Molecular Sciences, 25*(23), 12613.

Ullah, A., Sun, Q., Li, J., Li, J., Khatun, P., Kou, G., & Lyu, Q. (2024). Bioactive compounds in *Citrus reticulata* peel are potential candidates for alleviating physical fatigue through a triad approach of network pharmacology,

molecular docking, and molecular dynamics modeling. *Nutrients, 16*(12), 1934.

Verma, V. S. (2025). Development of multi-target directed ligands for neurodegenerative disorders: A medicinal chemistry approach. *Interconnected Journal of Chemistry and Pharmaceutical Sciences (IJCPS)*, 49–65.

Yang, Z., Zou, Y., & Wang, L. (2023). Neurotransmitters in prevention and treatment of Alzheimer's disease. *International Journal of Molecular Sciences, 24*(4), 3841.

Zhang, N., Chai, S., & Wang, J. (2025). Assessing and projecting the global impacts of Alzheimer's disease. *Frontiers in Public Health, 12*, 1453489.

Zhang, W., Lan, Y., Dang, B., Jin, H., Yang, X., & Li, Z. (2025). Identification and in vitro antioxidant and hypoglycemic activities of phenolic compounds in the different solvent fractions of polyphenols from black highland barley. *Journal of Food Measurement and Characterization, 19*(7), 4475–4488.